

Preparation, Characterization, and Crystal Structure of the Adducts $WF_6 \cdot F\text{-py}$ and $WOF_4 \cdot F\text{-py}$ ($F\text{-py} = 2\text{-Fluoropyridine}$)

Lucile Arnaudet, Roland Bougon,* Ban Buu, Monique Lance, Martine Nierlich, and Julien Vigner

SCM-URA 331 CNRS, CEA—Centre d'Etudes de Saclay, 91191 Gif-sur-Yvette, France

Received July 28, 1992

The adducts of tungsten(VI) $WF_6 \cdot F\text{-py}$ and $WOF_4 \cdot F\text{-py}$ have been prepared from the reaction of WF_6 or WOF_4 with 2-fluoropyridine ($F\text{-py}$) in dichloromethane. The two adducts were characterized by X-ray powder data and vibrational spectroscopy. The adduct of WOF_4 is only slightly volatile at room temperature, whereas that of WF_6 has a dissociation pressure of 26.5 mmHg at 21 °C. Solutions of these adducts in CD_2Cl_2 were studied by ^{19}F , 1H , and ^{13}C NMR spectroscopy. In $WOF_4 \cdot F\text{-py}$, the fluorine atoms bonded to the tungsten atom are magnetically equivalent, and their coupling with the fluorine atom of $F\text{-py}$ was observed at 25 °C ($\delta(F_w) = 66.8$ ppm/ $CFCl_3$, $J_{FF} = 14.3$ Hz). The labile character of $F\text{-py}$ in $WF_6 \cdot F\text{-py}$ did not permit such observations. The crystal structures of $WF_6 \cdot F\text{-py}$ and $WOF_4 \cdot F\text{-py}$ have been determined by X-ray diffraction methods. In $WF_6 \cdot F\text{-py}$, the tungsten atom is surrounded by a capped trigonal prism of ligands with the nitrogen atom of the organic ligand occupying the capping site. In $WOF_4 \cdot F\text{-py}$, the tungsten atom is surrounded by a distorted octahedron of ligands with the nitrogen atom of the organic ligand trans to the oxygen atom and the equatorial plane made up of four fluorine atoms located at the corners of a square. The space groups, unit cell parameters, and R factors are as follows. $WF_6 \cdot F\text{-py}$: monoclinic, $P2_1/c$ (No. 14), $a = 7.008(9)$ Å, $b = 15.373(3)$ Å, $c = 8.023(3)$ Å, $\beta = 101.62(4)^\circ$, $V = 846(1)$ Å³, $Z = 4$, $R = 0.028$. $WOF_4 \cdot F\text{-py}$: monoclinic, $P2_1/c$ (No. 14), $a = 8.742(3)$ Å, $b = 9.349(8)$ Å, $c = 10.737(4)$ Å, $\beta = 106.85(3)^\circ$, $V = 840(1)$ Å³, $Z = 4$, $R = 0.033$.

Introduction

Fluorides and oxide fluorides of transition elements such as tungsten(VI) or molybdenum(VI) are known to be good electron acceptors.¹ Depending on the nature of the base, and/or reaction conditions, either ionic or molecular species are obtained. As far as organic bases are concerned, they must, of course, be resistant to fluorinating attack by the fluoride or oxide fluoride. The strong nitrogen base pyridine (py) combined with the hexafluoride (WF_6) or the oxide tetrafluoride (WOF_4) of tungsten has been found to fulfill this condition.^{1,2} The structures of the adducts obtained with WOF_4 ($WOF_4 \cdot 2py$ and $WOF_4 \cdot py$) have been determined, and the coordination polyhedron of the tungsten atom has been shown to be a pentagonal bipyramid and a distorted octahedron in $WOF_4 \cdot 2py$ and $WOF_4 \cdot py$, respectively.¹ The effect of the number and nature of the ligands on the stereochemistry of this type of coordination compounds was further investigated by using an organic base that could give insight into their structure in solution. 2-Fluoropyridine ($F\text{-py}$), the properties of which are similar to those of py ,³ was chosen because its fluorine atom constituted an internal probe that could facilitate the study in solution by NMR spectroscopy. The behavior of this base toward WOF_4 and WF_6 was investigated. The interest in using WF_6 as a coordinating molecule was not only to alter the number of ligands with respect to that of the WOF_4 adducts but also to obtain for the first time solid-state structural information on a molecular adduct of WF_6 .

Experimental Section

Apparatus. Volatile fluorides were manipulated in an all-metal vacuum line, which was passivated with chlorine trifluoride prior to its use. Other volatile materials were purified and transferred in a glass vacuum line designed to handle moisture-sensitive materials. Solid products were handled in the dry argon atmosphere of a glovebox (Braun). Infrared spectra were recorded in the range 4000–200 cm^{-1} on a Perkin-Elmer

Table I. Crystallographic Data for $WF_6 \cdot F\text{-py}$ and $WOF_4 \cdot F\text{-py}$

	$WF_6 \cdot F\text{-py}$ ($C_5H_4F_7NW$)	$WOF_4 \cdot F\text{-py}$ ($C_5H_4F_5NOW$)
fw	394.93	372.93
space group	$P2_1/c$ (No. 14)	$P2_1/c$ (No. 14)
a , Å	7.008(9)	8.742(3)
b , Å	15.373(3)	9.349(8)
c , Å	8.023(3)	10.737(4)
β , deg	101.62(4)	106.85(3)
V , Å ³	846(1)	840(1)
Z	4	4
T , K	295	295
λ , Å	0.710 73	0.710 73
μ , cm^{-1}	140.13	140.96
ρ_{calc} , $g\ cm^{-3}$	3.098	2.949
transm coeff	0.840, 1.278	0.809, 1.336
$R(F_o)^a$	0.028	0.033
$R_w(F_o)^b$	0.035	0.041

$$^a R(F) = \frac{\sum |F_o| - |F_c|}{\sum |F_o|}, \quad ^b R_w(F) = \frac{[\sum w(|F_o| - |F_c|)^2 / \sum w |F_o|^2]^{1/2}}$$

Model 283 spectrophotometer. Spectra of solids were obtained by using small crystals pressed between AgBr windows in an Econo press (Barnes Engineering Co.). A standard cell, equipped with KBr windows, and a Monel cell of 10-cm path length equipped with AgCl windows were used for liquids and gases, respectively. Raman spectra of polycrystalline materials or liquids contained in 5 mm o.d. glass tubes were recorded on a Coderg Model T 800 spectrophotometer using the 514.5-nm exciting line of an Ar ion Model 2016 Spectra Physics laser filtered with a Coderg premonochromator. Low-temperature Raman spectra were recorded at -196 °C with the sample mounted in an unsilvered Pyrex dewar filled with liquid nitrogen. The NMR spectra were recorded on a Bruker Model AC 200 spectrometer at 200.13, 188.3, and 50.32 MHz for 1H , ^{19}F , and ^{13}C , respectively. Samples were referenced externally with respect to $Si(CH_3)_4$ or $CFCl_3$, with positive shifts being downfield from the standards. Elemental analyses were performed by Mikroanalytische Laboratorien, Elbach, Germany.

X-ray Diffraction. X-ray powder diffraction patterns of the samples sealed in 0.5 mm o.d. quartz capillaries were obtained by using a Philips camera (diameter 11.46 cm) with Ni-filtered $Cu\ \alpha$ radiation. Crystals suitable for structure determination were selected in the drybox under a microscope and sealed inside 0.5 mm o.d. quartz capillaries. X-ray diffraction was carried out on an Enraf-Nonius CAD 4 automated diffractometer. Cell dimensions were obtained by a least-squares

(1) Arnaudet, L.; Bougon, R.; Buu, B.; Charpin, P.; Isabey, J.; Lance, M. *Inorg. Chem.* **1989**, *28*, 257 and references therein.

(2) Tebbe, F. N.; Muetterties, E. L. *Inorg. Chem.* **1968**, *7*, 172.

(3) Muetterties, E. L. *Advances in the Chemistry of the Coordination Compounds*; Macmillan: New York, 1961; p 509.

Table II. Raman Data^a for WF₆-F-py and WOF₄-F-py and Comparison with Those for F-py

F-py ^b	WF ₆ -F-py ^c	WOF ₄ -F-py ^c	main assignments ^d	F-py ^b	WF ₆ -F-py ^c	WOF ₄ -F-py ^c	main assignments ^d	
	74		lattice modes	827	843	837	X-sensitive (r)	
	88			840				
	112				885	886		
	128	154				1006	W=O str	
	171	167		WF ₆ and WOF ₄ def modes				
	197				994	1029	1024	sym ring def (p)
	207	218			1044	1068	1064	β(C-H) (b)
230	233			X-sensitive (x)	1097	1117	1111	β(C-H) (d)
	272	262			1143	1166	1162	β(C-H) (a)
	307	311				1244	1254	
	320		WF ₆ and WOF ₄ def modes	1247	1295	1282	X-sensitive (q)	
	330			1303	1310	1314	β(C-H) (e)	
	339			1470	1490	1490	ν(C-C, C-N) (m)	
420	372		φ(C-C) (w)	1573 sh	1574	1570		
434	434	440		1580		1582	ν(C-C) (l)	
	468 sh			1598			ν(C-C) (k)	
	475			1617	1625	1618		
518	520	520		2936				
556	565	561	X-sensitive (t)	3026				
622	604	614	α(C-C-C) (s)	3071		3074	ν(C-H) (z ₁)	
	633			3092 sh	3099	3098	ν(C-H) (z ₂) (z ₅)	
	646	640	W-F str modes		3112	3117		
	662	662			3133			
	712	702	sym W-F str	3152	3144			
736		741	φ(C-C) (v)	3191				
786		787	γ(C-H) (f)	3208				

^a Frequencies in cm⁻¹ with those of the most intense bands in italics; sh = shoulder, sym = symmetric, def = deformation. ^b Liquid at room temperature. ^c Crystals at -196 °C. ^d The main assignments for F-py are from ref 9. Letters in parentheses are the code letter designations for the vibrations of the organic ligand.¹⁰ The X-sensitive modes^{9,10} are those in which the substituent X (here X = F) moves with appreciable amplitude.

refinement of the setting angles of the 25 reflections with θ between 8 and 12°. Intensities were corrected for Lorentz-polarization effects. The structures were solved by the heavy-atom method and refined by full-matrix least-squares techniques (F). The tungsten atoms in both adducts and the oxygen atom in WOF₄-F-py were refined anisotropically; all other atoms were refined isotropically. DIFABS⁴ was used to correct intensities for absorption. All calculations were performed on a Micro Vax II computer using the Enraf-Nonius structure determination package.⁵ Analytical scattering factors for neutral atoms⁶ were corrected for both $\Delta f'$ and $\Delta f''$ components of anomalous dispersion. Other experimental details appear with the crystal data in Table I and in the supplementary material.

Materials. Tungsten hexafluoride from Comurhex was purified by storage over sodium fluoride pellets. Tungsten oxide tetrafluoride was obtained as described in the literature⁷ and purified by sublimation under dynamic vacuum at ca. 50 °C. 2-Fluoropyridine, CH₂Cl₂ (both from Prolabo), and CD₂Cl₂ (CEA; 99.3% isotopic enrichment) were dried over P₂O₅.

Preparation of WF₆-F-py. In a typical preparation, 9.37 mmol of F-py was condensed into a glass flask cooled at -196 °C that had been evacuated on the vacuum line. An amount of 4 cm³ of CH₂Cl₂ was then added by condensation at this temperature. The mixture was warmed to room temperature, stirred for a few minutes, and cooled again to -196 °C; then 20.61 mmol of WF₆ was condensed onto it. Warming the solution to room temperature resulted in a pale yellow limpid solution. Cooling this solution to -50 °C gave a deposit of colorless crystals. Most of the solvent and excess WF₆ were removed by decantation at this temperature. The product was finally dried in vacuo at -25 °C for a few hours. Anal. Calcd for WF₆-F-py: W, 46.57; F, 33.68; C, 15.19; H, 1.01; N, 3.54. Found: W, 46.50; F, 33.51; C, 15.48; H, 1.00; N, 3.60.

Preparation of WOF₄-F-py. The reaction was run as for WF₆-F-py except that WOF₄ was loaded in the drybox into the dried glass flask. The solvent and F-py were then successively condensed into the flask at -196 °C with warming to room temperature and stirring between the two

additions. Decantation and in vacuo drying were achieved at -30 °C. Contrary to WF₆-F-py, the product is not labile in CH₂Cl₂ at room temperature; hence, the WOF₄/F-py molecular ratio could be determined by ¹⁹F NMR spectroscopy. The ratio of the integrated areas of the F-on-W and F-on-C signals was found to be equal to 1.

Results and Discussion

Syntheses and Properties of the Adducts WF₆-F-py and WOF₄-F-py. Tungsten hexafluoride and F-py react in dichloromethane to yield an adduct which, according to the NMR results (see below), is labile down to -40 °C in this solvent. In the range of concentration that was used, the solution had to be cooled to -50 °C to obtain the adduct with a sufficient yield. In a similar way, WOF₄ reacts with F-py to yield only a one-to-one adduct. The use of up to a 5-fold excess of F-py did not lead to a different molecular ratio in the product obtained.

Both adducts are extremely moisture sensitive. The adduct of WF₆ has a dissociation pressure of 26.5 mm at 21 °C. The infrared spectrum of the vapor above the solid at this temperature showed only the bands of WF₆ and F-py. The adduct of WOF₄ is only slightly volatile at room temperature, and its dissociation pressure could not be measured with the available equipment. Unlike the case of the analogous systems WF₆/py and WOF₄/py, for which the adducts WF₆-2py and WOF₄-2py have been obtained,^{1,2} no such extracoordination was achieved with F-py as a ligand. This, obviously, is related to the reduced basicity of F-py compared with that of py.

Vibrational Spectra. The Raman and infrared spectra of WOF₄-F-py were obtained, but owing to the easy dissociation of WF₆-F-py, no satisfactory infrared spectrum could be obtained for this adduct with the equipment available. Consequently, since they were sufficient for the discussion presented here, only Raman data are shown in Table II. As far as vibrations originating from those of WF₆ and WOF₄ are concerned, a striking feature brought about by the donor-acceptor interaction is a decrease in the W=O and symmetric W-F stretching frequencies: ν(W=O) 1058 cm⁻¹ in WOF₄¹¹ vs 1006 cm⁻¹ in WOF₄-F-py; symmetric ν(W-F)

- (4) Walker, N.; Stuart, D. *Acta Crystallogr.* **1983**, *A39*, 158.
- (5) *MolEN: An Interactive Structure Solution Procedure*; Enraf-Nonius: Delft, The Netherlands, 1990.
- (6) *International Tables for X-ray Crystallography*; Kynoch: Birmingham, England, 1974; Vol. IV.
- (7) Wilson, W. W.; Christie, K. O. *Inorg. Synth.* **1986**, *24*, 37.
- (8) Johnson, C. K. ORTEP II. Report No. ORNL 5138; Oak Ridge National Laboratory: Oak Ridge, TN, 1976.
- (9) Abdel-Shafy, H.; Perlmutter, H.; Kimmel, H. *J. Mol. Struct.* **1977**, *42*, 37.
- (10) Whiffen, D. H. *J. Chem. Soc.* **1956**, 1350.

- (11) Alexander, L. E.; Beattie, I. R.; Bukovszky, A.; Jones, P. J.; Marsden, C. J.; Van Schalkwyk, G. J. *J. Chem. Soc., Dalton Trans.* **1974**, 81.

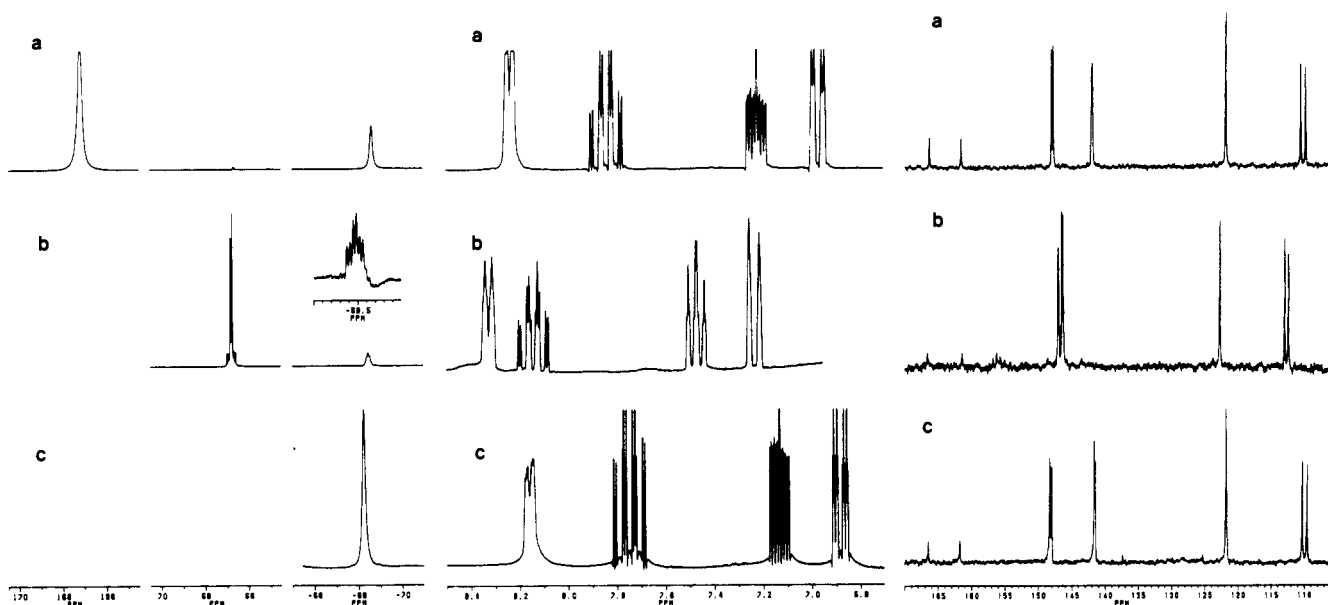
Table III. NMR Data^a for Solutions of WF₆-F-py and WOF₄-F-py in CD₂Cl₂ and Comparison with Those for F-py

	¹ H													
	δ ₃	δ ₄	δ ₅	δ ₆	J _{F,H₁}	J _{F,H₂}	J _{F,H₃}	J _{F,H₄}	J _{H₁,H₂}	J _{H₁,H₃}	J _{H₁,H₄}	J _{H₂,H₃}	J _{H₂,H₄}	J _{H₃,H₄}
F-py	6.88	7.75	7.13	8.16	2.69	8.26	2.46	0	8.27	0.87	0.82	7.25	2.09	4.88
WOF ₄ -F-py	7.23	8.14	7.47	8.33	0	7.0	1.2	0	8.5	1.2	0	7.1	2.0	5.8
WF ₆ -F-py	6.97	7.84	7.23	8.24	2.3	8.2	2.2	0	8.2	0.9	0.9	7.3	2.0	4.9

	¹⁹ F						¹⁹ F		
	δ _{F_W}	J _{WF_W}	J _{F_W,F₂}	δ _{F₂}	J _{F₂,F_W}	J _{F₂,H₂}	δ _{F_W}	δ _{F₂}	
F-py				-68.24			WF ₆ -F-py	167.20	-68.63
WOF ₄ -F-py	66.77	62.4	14.3	-68.47	14.4	7.2			

	¹³ C													
	δ ₂	δ ₃	δ ₄	δ ₅	δ ₆	J _{C₂,F₂}	J _{C₁,F₂}	J _{C₁,F₂}	J _{C₁,F₂}	J _{C₁,F₂}	J _{C₁,H₁}	J _{C₁,H₂}	J _{C₁,H₃}	J _{C₁,H₄}
F-py	164.10	109.90	141.54	121.71	148.13	237.27	37.31	7.9	3.95	14.68	170	164	166	188
WOF ₄ -F-py	163.99	112.65	146.37	122.67	146.98	261.6	29.24	10.1	3.8	8.5	174	163	174	184
WF ₆ -F-py	163.94	110.15	141.95	121.77	147.87	239.43	36.55	7.73	3.68	13.63				

^a Chemical shifts δ in ppm from TMS for the nuclei ¹H and ¹³C and from CFCl₃ for ¹⁹F; coupling constants J in Hz; subscript 2 refers to the fluorine atom of F-py or to the carbon atom to which it is attached, subscript W refers to the fluorine atoms bonded to the tungsten atom; subscripts 3–6 refer to hydrogen or carbon atom positions, with 3 indicating the position adjacent to the carbon atom that is bonded to the fluorine atom and 4–6 indicating positions para, meta, and ortho to the nitrogen atom, respectively. The ¹³C–¹H coupling constants for F-py and WOF₄-F-py were determined by the 2-D sequence "HETJRES" provided by Bruker.

**Figure 1.** NMR spectra of solutions of WF₆-F-py (a), WOF₄-F-py (b), and F-py (c) in CD₂Cl₂ at room temperature: left, ¹⁹F; middle, ¹H; right, ¹³C.

728 cm⁻¹ in WOF₄¹¹ vs 702 cm⁻¹ in WOF₄-F-py and 772 cm⁻¹ in WF₆ (crystal)¹² vs 712 cm⁻¹ in WF₆-F-py. These negative shifts in frequency are quite in line with a transfer of electronic density from the nitrogen lone pair to the tungsten atom. On the contrary, and for the same reason, among the vibration modes of the organic ligand, the so-called X-sensitive modes q, r, and t (see Table II), which are in-plane ring symmetric deformation modes, the in-plane symmetric ring deformation mode p, the in-plane C–H bending modes a, b, d, and e, and the mode m (C–C and C–N stretching hybrid mode) are all increased in the adducts. The overall trend indicates a ring configuration more rigid in the adducts than in the free ligand.

Nuclear Magnetic Spectra. The NMR spectra were recorded for the solutions of WOF₄, WF₆, F-py, WOF₄-F-py, and WF₆-F-py in CD₂Cl₂. At 25 °C, the ¹⁹F spectrum of WOF₄ showed a broad line (fwhm 715 Hz) at δ = 74.1 ppm, and that of WF₆ showed a line (fwhm 2.2 Hz) at δ = 166.7 ppm. The data for F-py, WOF₄-F-py, and WF₆-F-py appear in Table III. The ¹⁹F spectrum of WOF₄-F-py, shown in Figure 1, is of A₄MX type. It consists of a doublet at δ = 66.8 ppm and a doublet of quintets at δ = -68.5 ppm. The doublet corresponds to the four fluorine

atoms (A₄) bonded to the tungsten atom, which are rendered magnetically equivalent by the internal rotation around the W–N bond. The splitting into a doublet is due to the coupling of these fluorine atoms with that of F-py (M). The ¹⁸³W satellites are also observed. The doublet of quintets corresponds to the resonance of M split by A₄ and by the proton (X) of F-py in para position to the nitrogen atom. The doublet of quintets was changed into a quintet by irradiation of X. The correlation, which was found between A₄ and M by 2D COSY experiments, gave further support to the overall interpretation. The ¹H NMR spectrum of WOF₄-F-py, also shown in Figure 1, is similar to that of F-py, except that the lines are broader and shifted to higher frequency. This shift indicates a deshielding of the protons. To a less extent, this trend is also observed for the ¹³C NMR spectrum (Figure 1 and Table III). For both spectra the lines corresponding to the carbon and hydrogen atoms in positions para to the nitrogen atom are the most shifted. It is also noted that the coupling between the carbon and fluorine atoms in positions ortho to the nitrogen atom is stronger in WOF₄-F-py than in F-py.

The ¹H, ¹⁹F, and ¹³C spectra of WF₆-F-py at 25 °C (Table III and Figure 1) are not significantly changed from those of F-py and WF₆ taken separately. This indicates that the adduct is

Table IV. Positional Parameters and Their Estimated Standard Deviations

atom	<i>x</i>	<i>y</i>	<i>z</i>	<i>B</i> , Å ² ^a
WF ₆ -F-py				
W	0.14235(9)	-0.06030(4)	0.27431(7)	3.97(1)*
F	0.086(1)	-0.2721(6)	0.244(1)	6.3(2)
F(1)	0.145(1)	0.0583(6)	0.281(1)	6.9(2)
F(2)	-0.110(2)	-0.0270(8)	0.180(1)	8.2(3)
F(3)	0.365(1)	-0.0372(6)	0.193(1)	5.5(2)
F(4)	0.090(1)	-0.1277(6)	0.080(1)	5.0(2)
F(5)	0.005(1)	-0.1272(6)	0.392(1)	6.8(2)
F(6)	0.282(1)	-0.0387(6)	0.494(1)	6.5(2)
N	0.332(1)	-0.1820(7)	0.341(1)	3.1(2)
C(1)	0.276(2)	-0.2630(9)	0.312(2)	3.6(3)
C(2)	0.383(2)	-0.335(1)	0.349(2)	4.6(3)
C(3)	0.575(2)	-0.323(1)	0.427(2)	5.3(4)
C(4)	0.641(2)	-0.241(1)	0.460(2)	5.1(4)
C(5)	0.525(2)	-0.172(1)	0.416(2)	4.5(3)
H(2)	0.327	-0.391	0.322	6.0
H(3)	0.660	-0.371	0.457	6.0
H(4)	0.772	-0.232	0.517	6.0
H(5)	0.576	-0.115	0.436	6.0
WOF ₄ -F-py				
W	0.21527(9)	0.10353(9)	0.41742(8)	3.10(2)*
F	0.483(1)	0.290(1)	0.650(1)	5.2(3)
F(1)	0.271(1)	0.064(1)	0.591(1)	4.4(3)
F(2)	0.013(1)	0.155(1)	0.425(1)	4.9(3)
F(3)	0.163(1)	0.198(1)	0.256(1)	4.9(3)
F(4)	0.430(1)	0.120(1)	0.424(1)	4.9(3)
O	0.180(2)	-0.064(1)	0.362(2)	4.9(4)*
N	0.265(1)	0.346(2)	0.488(1)	2.8(3)
C(1)	0.379(2)	-0.388(2)	0.589(2)	2.5(4)
C(2)	0.409(2)	0.531(2)	0.632(2)	3.9(5)
C(3)	0.306(2)	0.629(2)	0.572(2)	4.3(5)
C(4)	0.175(2)	0.589(2)	0.455(2)	4.6(5)
C(5)	0.164(2)	0.448(2)	0.424(2)	3.4(4)

^a Asterisk denotes *B*_{eq} value, equal to $4/3 \sum_i \sum_j \beta_{ij} \bar{a}_i \bar{a}_j$.

dissociated in CD₂Cl₂. However, the average ¹⁹F signal of the fluorine atoms bonded to the tungsten atom (F_W) was shifted to higher frequency upon cooling ($\delta = 169.4$ and 170.5 ppm at 0 and -30 °C, respectively) and split into two broad lines ($\delta = 176.8$ ppm (fwhm 520 Hz) and 167.1 ppm (fwhm 520 Hz)) at -40 °C. The proton lines were also found to be shifted to higher frequency upon cooling, to reach at -40 °C δ values close to those found for WOF₄-F-py at 25 °C. The ¹⁹F signal at 167.1 ppm was assigned to "free" WF₆ (for WF₆ in CD₂Cl₂ at -40 °C without F-py, $\delta = 166.6$ ppm (fwhm 1.6 Hz)) and that at $\delta = 176.8$ ppm to WF₆ bonded to F-py. Another interpretation would have consisted of assigning these lines to two types of fluorine atoms in the adduct, as found, for instance, in the crystal. However, this interpretation is not justified owing to the variable intensity ratios, which were found for these two lines. The broadness of these lines indicates that there is an exchange of the F-py ligand between WF₆ molecules and that this exchange takes place down to the lowest temperature (-70 °C) which could be reached. Surprisingly, the shift to higher frequency that was observed for the atoms F_W in the adduct is not in agreement with the expected global increase of their shielding.

Crystal Structures. The molecular stereochemistry of the adducts WF₆-F-py and WOF₄-F-py was established by single-crystal studies. Crystal data are given in Table I. Final positional and thermal parameters are given in Table IV with their standard deviations. The relevant distances and angles are given in Table V. Figure 2 shows the molecular unit and atomic labeling scheme for WF₆-F-py and WOF₄-F-py. Figure 3 gives stereoscopic views of the molecular packing for WF₆-F-py and WOF₄-F-py. Both compounds are of molecular type, and their packing is governed by the pyridine rings, which lie in parallel planes. The coordination polyhedron of the tungsten atom in WF₆-F-py is a capped trigonal prism with the nitrogen atom of the organic ligand occupying the capping site. Fluorine atoms F(1) and F(2), the tungsten atom, and F-py are in the same plane ($\pm 0.02(1)$ Å). This plane is

Table V. Selected Bond Lengths (Å) and Angles (deg)

WF ₆ -F-py		WOF ₄ -F-py	
W-F(1)	1.824(8)	W-F(1)	1.82(1)
W-F(2)	1.85(1)	W-F(2)	1.857(9)
W-F(3)	1.842(7)	W-F(3)	1.88(1)
W-F(4)	1.844(7)	W-F(4)	1.868(9)
W-F(5)	1.803(8)	W-O	1.68(1)
W-F(6)	1.863(8)	W-N	2.39(1)
W-N	2.294(9)		
F(1)-W-F(2)	74.8(4)	F(1)-W-F(2)	89.1(4)
F(1)-W-F(3)	79.2(3)	F(1)-W-F(3)	163.6(5)
F(1)-W-F(4)	125.8(3)	F(1)-W-F(4)	90.6(4)
F(1)-W-F(5)	123.9(4)	F(1)-W-O	98.2(5)
F(1)-W-F(6)	78.2(3)	F(1)-W-N	84.1(5)
F(1)-W-N	143.8(3)	F(2)-W-F(3)	86.5(5)
F(2)-W-F(3)	127.7(4)	F(2)-W-F(4)	159.8(4)
F(2)-W-F(4)	78.5(4)	F(2)-W-O	100.3(5)
F(2)-W-F(5)	78.7(4)	F(2)-W-N	80.1(4)
F(2)-W-F(6)	127.8(4)	F(3)-W-F(4)	88.1(4)
F(2)-W-N	141.4(4)	F(3)-W-O	98.2(6)
F(3)-W-F(4)	81.3(3)	F(3)-W-N	79.5(4)
F(3)-W-F(5)	151.2(4)	F(4)-W-O	99.7(5)
F(3)-W-F(6)	88.8(4)	F(4)-W-N	79.7(4)
F(3)-W-N	75.5(3)	O-W-N	177.6(6)
F(4)-W-F(5)	95.0(4)		
F(4)-W-F(6)	151.0(4)		
F(4)-W-N	75.4(4)		
F(5)-W-F(6)	80.7(4)		
F(5)-W-N	75.9(3)		
F(6)-W-N	75.8(3)		

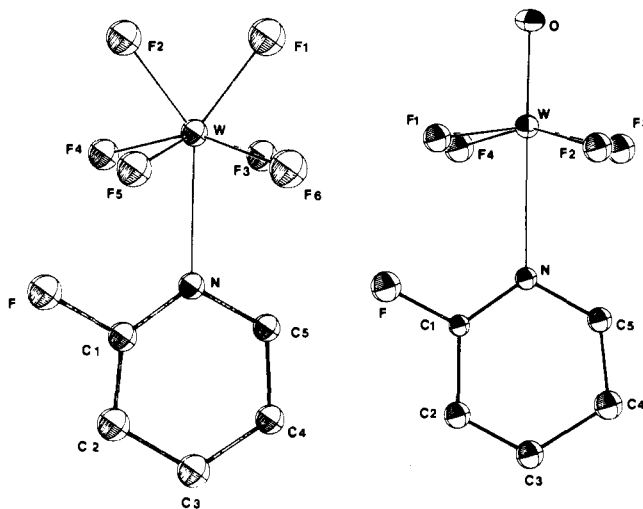


Figure 2. ORTEP⁸ drawings of the molecular units WF₆-F-py (left) and WOF₄-F-py (right) with the hydrogen atoms omitted. Vibration ellipsoids are drawn at the 30% probability level.

perpendicular to the plane made up of fluorine atoms F(3), F(4), F(5), and F(6), and its projection is parallel to the F(3)-F(4) and F(5)-F(6) edges. The tungsten atom is displaced 0.456(1) Å out of the plane F(3)-F(4)-F(5)-F(6) toward the F(1)-F(2) edge.

The coordination polyhedron of the tungsten atom in WOF₄-F-py is a distorted octahedron with the nitrogen atom of the organic ligand being trans to the oxygen atom and the equatorial plane made up of four fluorine atoms located at the corners of a square. The tungsten atom is displaced 0.294(1) Å out of this plane toward the oxygen atom. The oxygen and nitrogen atoms are in apical positions, and the O-W-N axis, almost linear (177.6(6)°), is perpendicular to the equatorial plane. The F-py plane is perpendicular to the equatorial plane with its projection parallel to the F(1)-F(2) and F(3)-F(4) edges.

As expected, the molecular structures of WOF₄-F-py and WOF₄-py¹ are quite alike. The few differences which were observed may be interpreted as being due to the reduced force of the base F-py compared with that of py. The lower electronic density brought in to the tungsten atom in WOF₄-F-py results in

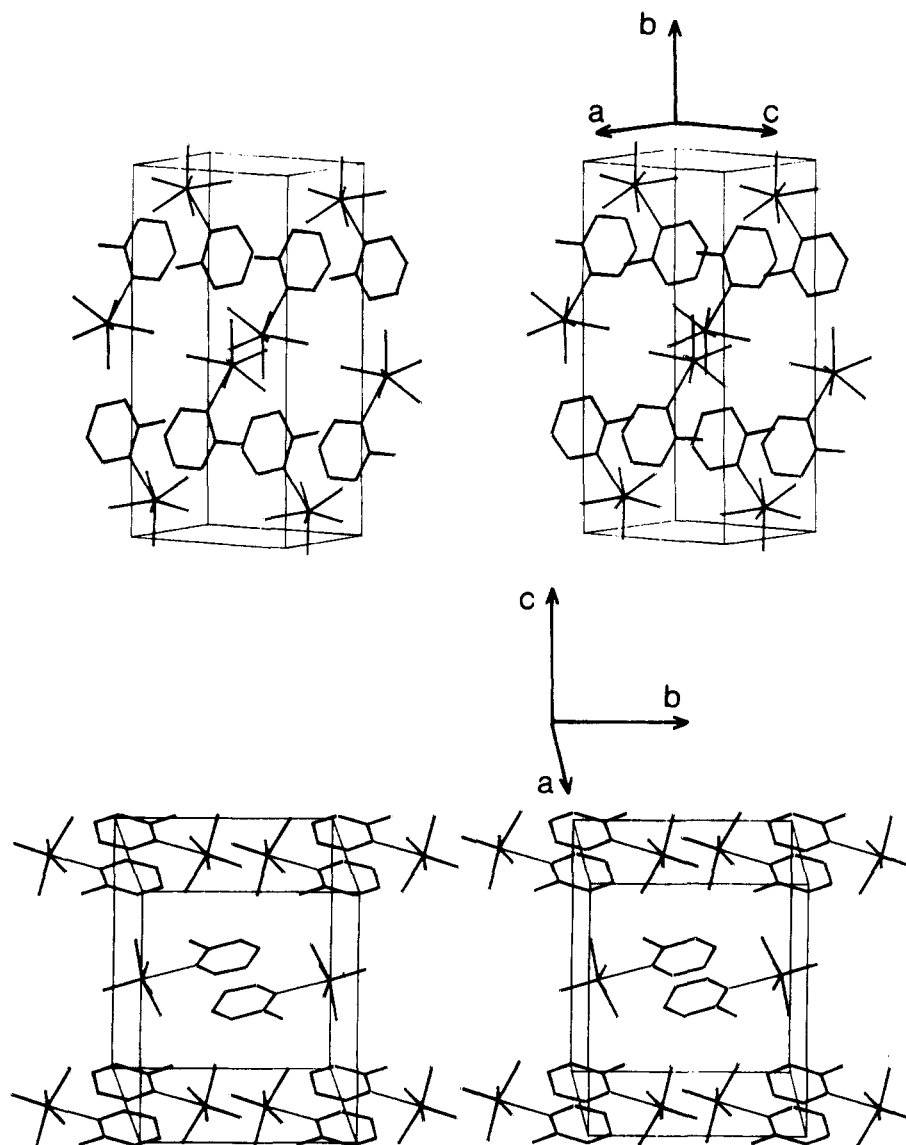


Figure 3. Stereoscopic views of the structure in the unit cell of $\text{WF}_6 \cdot \text{F-py}$ (top) and $\text{WOF}_4 \cdot \text{F-py}$ (bottom).

a strengthening of the $\text{W}=\text{O}$ bond (distances 1.68(1) and 1.77(5) Å and vibration frequencies 1006 and 996 cm^{-1} for $\text{WOF}_4 \cdot \text{F-py}$ and $\text{WOF}_4 \cdot \text{py}$, respectively). From this shortening of the $\text{W}=\text{O}$ bond, its repulsive effect on the fluorine atoms of the equatorial plane is more pronounced in $\text{WOF}_4 \cdot \text{F-py}$ than in $\text{WOF}_4 \cdot \text{py}$. The displacements of the tungsten atoms out of the equatorial planes are found to be 0.294(1) and 0.280(1) Å for $\text{WOF}_4 \cdot \text{F-py}$ and $\text{WOF}_4 \cdot \text{py}$, respectively.

Conclusion. Two new adducts of tungsten(VI) have been prepared and characterized. It has been demonstrated from X-ray structure determination, Raman spectroscopy, and NMR spectroscopy that these two adducts are of molecular type, with the F-py molecule bound to the tungsten atom through the nitrogen atom. $\text{WF}_6 \cdot \text{F-py}$ is the first crystallographically characterized molecular adduct of WF_6 . The heptacoordination of the tungsten

atom in this adduct adopts the geometry of a capped trigonal prism. The few differences observed between the structural data of $\text{WOF}_4 \cdot \text{F-py}$ and those previously obtained for $\text{WOF}_4 \cdot \text{py}$ ¹ are explained by the reduced basicity of F-py compared with that of py . It is noted that the two adducts containing a 7-fold coordinated tungsten atom ($\text{WF}_6 \cdot \text{F-py}$ and $\text{WOF}_4 \cdot 2\text{py}$ ¹) easily dissociate and that the adduct of WF_6 is the less stable.

Acknowledgment. The assistance of Jacques Isabey with some technical aspects of this work is much appreciated.

Supplementary Material Available: Tables of crystal data, bond distances, bond angles, atomic positional parameters, and anisotropic thermal parameters (6 pages). Ordering information is given on any current masthead page.